MULTIPLE SCATTERING CONTRIBUTION TO TRABECULAR BONE BACKSCATTER

JANUSZ WÓJCIK, JERZY LITNIEWSKI, ANDZEJ NOWICKI

Institute of Fundamental Technological Research, Polish Academy of Sciences
Świętokrzyska 21, 00-049 Warsaw, Poland
Jwojcik@ippt.gov.pl

Integral equations that describe scattering on the structure with step rise parameters, have been numerically solved on example of the trabecular bone model. The model consists of several hundred elements with randomly selected parameters. The spectral distribution of scatter coefficients in subsequent orders of scattering has been presented.

INTRODUCTION

The evaluation of bone strength requires not only the knowledge of its mean density but also of its microscopic structure. The ultrasound signals that have been scattered in trabecular bone contain information of the properties of the bone structure, and hence the analysis of the backscatter could be useful in assessment of the microscopic architecture of the bone. It has been demonstrated that the use of the backscattering models of bone enabled an assessment of some micro-structural characteristics from the experimental data.

Starting from Wear's work [1], the best of the authors' knowledge almost all of the reported bone scattering models assumed, not precisely speaking the Born approximation, and consequently the multiple scattering within the bone trabeculae, was neglected. Trabecular bone consists of trabeculae whose mechanical properties differ significantly from the surrounding marrow and therefore the ultrasonic wave is strongly scattered. The work of Bossey et al.[2] presents analytically advanced approach. The scattering structure corresponds to the real one. Unfortunately this approach does not enable determination of the influence of multiple scattering on total The field. The Wear's [3] work contains the review of methods and problems of bone sonometry.

The aim of the presented paper was the evaluation of the contribution of the first, second and higher order scattering (multiple scattering) into total scattering of the ultrasounds in the trabecular bone. The scattering, due to interconnections between thick trabeculae, usually neglected in trabecular bone models, has been also studied. Our model is fully scaled.

The basic element in our model of trabecular bone was an elastic cylinder with varying finite-length and diameter as well as orientation. The density and speed of sound were similar to those of the bone tissue. The cylinder was applied in building of the multi-element structures, similar to the architecture of the trabecular bone, taking into account variation of elements size and spatial configuration. The field scattered on the bone model was evaluated by solving numerically the integral form of the Sturm-Liouville equation in the version that describes longitudinal wave in inhomogeneous media.

For the calculated scattered fields the effective cross-sections as well as the Broadband Ultrasonic Backscatter (BUB), directly related to the detected echo-signal level, were determined. Calculations were performed for the frequency ranging from 0.5 to 3 MHz.

1. BASIC EQUATIONS

Lame's equation for longitudinal disturbances of stress in non-homogeneous and isotropic medium can be written as [4]

$$g\nabla\cdot\left(\frac{\nabla P}{g}\right)-\frac{1}{c^2}\partial_{tt}P-2\mathbf{A}\partial_t P=0\ , \tag{1}$$

where: $P=P(\mathbf{x},t)$ is normalized stress: $g=g(\mathbf{x})$, $c=c(\mathbf{x})$ are respectively: normalized density and speed of sound of the longitudinal waves, $(\mathbf{x},t)$ are normalized coordinates in space and time, whereas $\nabla,\nabla\cdot,\partial_t$ are normalized operators of gradient, divergence and derivation in respect to time. The normalization was performed as follows: $P\equiv\overline{P}/P_0$, $g\equiv\overline{g}/g_0$, $c\equiv\overline{c}/c_0$, $\mathbf{x}\equiv K_0\,\bar{\mathbf{x}}$, $t\equiv\omega_0\,\bar{t}$, $\nabla\equiv\overline{\nabla}/K_0$, $\partial_t\equiv\partial_{\bar{t}}/\omega_0$. P_0 is the reference pressure; g_0, c_0 are density and speed of sound in reference medium respectively (in our case - volume dominant reference). It means that $c=1$ and $g=1$ for reference medium. The dimensional variables are accented. The characteristic wave number K_0 and pulsation ω_0 are restricted by the relation: $K_0c_0=\omega_0$. $\omega_0\equiv 2\pi/T_0$, where T_0 is reference time (e.g. Time window). A consequence of the applied normalization method is equality of non-dimensional pulsation $n\equiv\omega/\omega_0$ and frequency *n,* and the wave number $k(n)=\pm n$ in dispersion less media. Most often for solid body Eq.(1) is written for displacement vector $\boldsymbol{\zeta}(\mathbf{x},t)$. The equation (1) was derived on the basis of the relation $P=\lambda\nabla\cdot\boldsymbol{\zeta}$ and $c^2=\lambda/g$. $\mathbf{A}$ is the convolution type operator describing the absorption [5]. We assume that for solid state $\mathbf{A}\equiv 0$. So called absorption coefficient $a(n)$ is a eigen value $\mathbf{A}$ for the eigen function $\exp(i\cdot n\cdot t)$, that means $a(n)=\mathrm{F}[A(t)]$, where $\mathrm{F}[\bullet]$ is the Fourier transform of time, while $A(t)$ is the kernel of $\mathbf{A}$. In dimensional units $\bar{a}=K_0 a$. After Fourier transform respect time, the Eq.(1) can be written as follows:

$$\Delta C+k^2C=\mathrm{V}C+\mathbf{Q}\cdot\nabla C,\qquad C=C(\mathbf{x},n)=\mathrm{F}[P(\mathbf{x},t)], \tag{2}$$

$$\mathrm{V}(\mathbf{x})\equiv n^2\left(1-\frac{1}{c(\mathbf{x})^2}\right)\qquad\qquad \mathbf{Q}(\mathbf{x})\equiv\frac{\nabla g}{g} \tag{3}$$

Complex wave number k is given by $k(n) \equiv \pm n\sqrt{1+i2\,a(n)/n} \cong \pm n + ia(n)$. Eq.(2) was written when Helmholtz operator $\Delta + k^2$ was distinguished for dominant reference medium surrounding regions of material parameter disturbances. Eq.(3) is based on the assumption that only in reference medium $a(n) \neq 0$.

2. MEDIUM CONSTRUCTION AND POTENTIALS.

We assume that reference medium surrounds L regions υ_l of space. The regions are bounded by surfaces s_l $l = 1,...,L$. We suppose that the υ_l are open sets in space, however $\overline{\upsilon_l} = \upsilon_l \cup s_l$ are closed. Each region $\overline{\upsilon_l}$ is filled with homogeneous medium and its density $g_l = const \neq 1$, as well as sound speed $c_l = const \neq 1$. The multiple-theory sum of the υ_l sets describes the structure being submerged in reference medium. We assume that elements of structure do not cross in a sense of 3D measure of volume $d^3(\cdot)$.

$$\upsilon = \bigcup_l \upsilon_l \quad , \; s = \bigcup_l s_l \;, \quad d^3(\upsilon_l \cap \upsilon_m) = 0 \tag{4}$$

Thus spatial distributions of sound speed and density have a form:

$$c(\mathbf{x})^2 = 1 + \sum_l \mathrm{d}c_l(\mathbf{x})^2 = 1 + \sum_l \chi_l (c_l^{\,2} - 1) \tag{5}$$

$$g(\mathbf{x}) = 1 + \sum_l \mathrm{d}g_l(\mathbf{x}) = 1 + \sum_l \chi_l (g_l - 1) \tag{6}$$

where $\chi_l \equiv \chi(\overline{\upsilon_l})$ is the characteristic function of υ_l, $\chi = 1$ for $\mathbf{x} \in \upsilon_l$, $\chi = 0$ for $\mathbf{x} \notin \upsilon_l$, $\chi = 1/2$ for $\mathbf{x} \in s_l$. The characteristic function of structure is $\chi(\upsilon) = \sum_l \chi(\upsilon_l)$.

The characteristic functions χ_l can also be defined in the following way: $\chi_l(\mathbf{x}) \equiv \chi(S_l(\mathbf{x}))$, where $S_l(\mathbf{x})$ satisfies the following conditions: $S_l(\mathbf{x}) = 0$ for $\mathbf{x} \in s_l$ surface equation s_l, $S_l(\mathbf{x}) \geq 0$ for $\mathbf{x} \in \overline{\upsilon_l}$, $S_l(\mathbf{x}) < 0$ for $\mathbf{x} \notin \overline{\upsilon_l}$. Taking into account that χ is the Hewisaid's distribution we obtain: $\chi(S_l) = 1$ for $S_l > 0$ and $\chi(S_l) = 0$ for $S_l < 0$.
Because $\partial_S \chi(S_l) = \delta(S_l)$, where $\delta(\cdot)$ is the Dirack distribution, then:

$$\nabla \mathrm{d}g_l(\mathbf{x}) = (1 - g_l)\delta(S_l(\mathbf{x}))\nabla S_l(\mathbf{x}) = (g_l - 1)\delta(S_l(\mathbf{x}))\mathbf{u}_l(\mathbf{x}) \tag{7}$$

Vector $\nabla \mathrm{d}g_l$ is normal to equiscalar surface δg_l and its length is inversely proportional to density. It is directed into growing values of $\mathrm{d}g$. Vector $\mathbf{u}_l(\mathbf{x}) \equiv -\nabla S_l(\mathbf{x})$ is externally normal to s_l in $\mathbf{x} \in s_l$ and is unit. Because $\mathbf{u}(\mathbf{x}) = \{\mathbf{u}_l(\mathbf{x}) : \mathbf{u}_l \perp s_l, l = 1,..., L\}$ is a general field of vectors being normal to the structure (surface $s = \cup s_l$), then:

$$\delta(S_l(\mathbf{x}))\mathbf{u}(\mathbf{x}) = \delta(S_l(\mathbf{x}))\mathbf{u}_l(\mathbf{x}) \tag{8}$$

since for $\mathbf{x} \notin s_l$ $\delta(S_l(\mathbf{x})) = 0$.
Thus, on the basis of the above considerations:

$$\nabla g(\mathbf{x}) = \sum_{l=1}^{L}(1-g_l)\delta(S_l(\mathbf{x}))\mathbf{u}_l(\mathbf{x}) = \left(\sum_{l=1}^{L}(1-g_l)\delta(S_l(\mathbf{x}))\right)\mathbf{u}(\mathbf{x}) \tag{9}$$

By neglecting detailed discussion, we can rewrite Eq.(9) in the form:

$$\nabla g(\mathbf{x}) = \left(\sum_{l=1}^{L}\sigma_l(1-g_l)\right)\delta(s)\mathbf{u}(\mathbf{x}) \tag{10}$$

where: $\delta(s) \equiv \sum_l \delta(S_l(\mathbf{x}))$, $\sigma_l(\mathbf{x}) \equiv 2\chi(\upsilon_l(\mathbf{x} \in s_l))$, $\sigma_l(\mathbf{x}) \equiv 2\chi(S_l(\mathbf{x}) = 0)$. Finally, we have

$$\mathbf{Q} \equiv \mathrm{Q}(\mathbf{x})\mathbf{u}(\mathbf{x})\delta(\mathrm{s}) = \left(\sum_l \sigma_l\left(\frac{1}{g_l}-1\right)\right)\mathbf{u}(\mathbf{x})\delta(s) = \left(\sum_l \mathrm{Q}_l\right)\mathbf{u}(\mathbf{x})\delta(s) \tag{11}$$

$$\mathrm{V} \equiv \sum_l \chi_l \mathrm{V}_l = \sum_l \chi_l n^2\left(1-\frac{1}{c_l^{\,2}}\right), \quad \mathrm{V} = \chi(\upsilon)\mathrm{V}. \tag{12}$$

3. SCATTERING EQUATIONS

For the assumed model of structure of medium the Eq.(2) takes the form

$$\Delta C + k^2 C = \mathrm{V}C + \mathrm{Q}B\delta(s), \quad B(\mathbf{x},n) \equiv \mathbf{u}(\mathbf{x}) \cdot \nabla C(\mathbf{x},n) \tag{13}$$

The field B is determined only on surface s of the structure υ. Further, if it will not make misunderstanding the non-dimensional pulsation will be neglected in the argument list. When transforming Eq.(13) into integral equation and using features of distributions $\delta(s)$ and $\chi(\upsilon)$ we obtain

$$\begin{aligned} C(\mathbf{x}) = C^0(\mathbf{x}) &- \int_{\upsilon} G(r(\mathbf{x},\mathbf{x}'))\mathrm{V}(\mathbf{x}')C(\mathbf{x}')d\upsilon \\ &- \int_{s} G(r(\mathbf{x},\mathbf{x}'))\mathrm{Q}(\mathbf{x}')B(\mathbf{x}')ds \end{aligned} \quad . \tag{14}$$

Where: $G(r,n) \equiv \exp(ik(n)r/4\pi r)$, $r = r(\mathbf{x},\mathbf{x}') = |\mathbf{r}|$, $\mathbf{r} = \mathbf{x} - \mathbf{x}'$, and $d\upsilon$ is a elementary volume in υ, ds is a elementary surface on s. $C^0(\mathbf{x}) \equiv C^0(\mathbf{x},n)$ is a solution of Helmholtz equation in reference medium (incident field), $G(r(\mathbf{x},\mathbf{x}')) = G(r(\mathbf{x},\mathbf{x}'),n)$ is the Green function of the Helmholtz equation . The integrals in Eq.(14) describe the scattering of incident field on potentials V and Q of the structure. It is sufficient to determine the equation for $\mathbf{x} \in \upsilon$ in order to solve it. When the solution is substituted to the integrals in Eq.(14) it gives solution in whole medium. Applying $\mathbf{u}(\mathbf{x}) \cdot \nabla$ to the both sides of Eq.(14) we get equation for the field B.

$$B(\mathbf{x}) = B^0(\mathbf{x}) - \int_{\upsilon} \partial G(r(\mathbf{x},\mathbf{x}'))\mathrm{V}(\mathbf{x}')C(\mathbf{x}')d\upsilon - \int_{s} \partial G(r(\mathbf{x},\mathbf{x}'))\mathrm{Q}(\mathbf{x}')B(\mathbf{x}')ds \quad , \quad \mathbf{x}\in\upsilon\,, s\subset\upsilon$$

(15)

$$B^0 = \mathbf{u}\cdot\nabla C^0\,,\ \ \partial G(r) = \mathbf{u}(\mathbf{x})\cdot\mathbf{e}(\mathbf{r})\partial_r G\,,\ \ \mathbf{e}(\mathbf{r}) = \nabla r = \mathbf{r}/r \tag{16}$$

By grouping the functions and their normal derivatives in vector function

$$\overline{\mathrm{C}} \equiv \begin{pmatrix} C \\ B \end{pmatrix},\ \overline{\mathrm{C}}^0 \equiv \begin{pmatrix} C^0 \\ B^0 \end{pmatrix},\ \overline{\mathrm{G}} \equiv \begin{pmatrix} G \\ \partial G \end{pmatrix},\ \mathrm{W} \equiv \begin{pmatrix} \mathrm{V}d\upsilon \\ \mathrm{Q}ds \end{pmatrix} \tag{17}$$

and introducing the scattering field $\mathrm{E} \equiv \overline{\mathrm{C}} - \overline{\mathrm{C}}^0$, we may rewrite Eqs.(14-15) in the compact form

$$(\mathbf{I} + \mathbf{GW})\mathrm{E} = -\mathrm{E}^0 \qquad \mathbf{GW}\overline{\mathrm{C}} \equiv \int (\overline{\mathrm{G}} \circ \mathrm{W})\overline{\mathrm{C}} \tag{18}$$

where, the kernel of operator $\mathbf{GW}$ is 2×2 matrices determined by diadic vectors product signs by $\circ$, $\mathrm{E}^0 = \mathbf{GW}\overline{\mathrm{C}}^0$. $\mathbf{I}$ is the identity operation $\mathbf{I}\mathrm{E}(\mathbf{x}') = \mathrm{E}(\mathbf{x})$. Equivalent form of the operator $\mathbf{GW}$ is

$$\mathbf{GW} \equiv \begin{pmatrix} \int d\upsilon \mathrm{V} G & \int ds \mathrm{Q} G \\ \int d\upsilon \mathrm{V}\partial G & \int ds \mathrm{Q}\partial G \end{pmatrix} \tag{19}$$

Integration domains are clearly determined by $d\upsilon$ and ds. Because $\mathrm{E} = \sum_l \chi_1 \mathrm{E} = \sum_1 \mathrm{E}_l$ then the operator $\mathbf{GW}$ can be presented as the sum of the cells $\mathbf{GW} = \cup_{l,m} \mathbf{GW}_{lm}$, where $\mathbf{GW}_{lm}$ is given by Eq.(18) or Eq.(19) for $\mathrm{W}_m = \chi_m \mathrm{W}$ and $\mathbf{x}\in\upsilon_l$. For $\mathbf{x},\mathbf{x}'\in\upsilon_l$ and $\mathbf{x} = \mathbf{x}'$, $\mathbf{GW}_{lm} = \mathbf{0}$ (no self interaction). We set $\mathbf{GW}_l \equiv \mathbf{GW}_{ll}$ for diagonal cells $l = m$.

4. SOLUTION METHOD

We seek the solution of Eq.(18) for $\mathbf{x}\in\upsilon$ in the form

$$\mathrm{E} = \sum_l \mathrm{E}_l^1 + \mathrm{R}^2 \tag{20}$$

where E_l^1 is the solution of Eq.(18) in *l- th* element of the structure under the assumption that the only scattering field in υ_l is $\mathrm{E}_l^0 = \chi_l \mathrm{E}^0$ produced by incident field $\overline{\mathrm{C}}_l^0 = \chi_l \overline{\mathrm{C}}^0$ $\mathrm{E}_l^0 = \mathbf{GW}_l \overline{\mathrm{C}}_1^0$.

$$(\mathbf{I} + \mathbf{GW}_l)\mathrm{E}_l^1 = -\mathrm{E}_l^0 \tag{21}$$

$$\mathrm{E}_l^1 = -\mathbf{H}_l \mathrm{E}_l^0 = -\mathbf{H}_l \mathbf{GW}_l \overline{C}_l^0 \qquad l = 1,\dots,L$$

where $\mathbf{H}_l \equiv (\mathbf{I} + \mathbf{GW}_l)^{-1}$ denotes inverse operator. The fields E_l^1 determine a field in medium in the first order of scattering (single scattering). The reminder R^2 denotes a field in structure created due to interaction between structure elements in the second and higher orders of the scattering (multi-scattering). The R^2 satisfies equation

$$(\mathbf{I} + \mathbf{GW})\mathrm{R}^2 = -\sum_l \mathbf{GW}_l \left(\sum_{m,m \neq l} E_m^1 \right) \qquad E_m^1 = \mathbf{GW}_{lm} \mathrm{E}_m^1 \tag{22}$$

The field E_m^1 is calculated as the field from the *m*- th element failing on *l*-th element. Then we repeat the described above procedure. We suppose that $\mathrm{R}^2 = \sum_l \mathrm{E}_l^2 + \mathrm{R}^3$ and E_l^2 satisfies Eq.(21) with source in the form of *l*-th component on right side in (22). Then we have

$$\mathrm{E}_l^2 = -\mathbf{H}_l \mathbf{GW}_l \sum_{m \neq l} E_m^1 , \tag{23}$$

and after substitution $E_m^2 \rightarrow E_m^1$ R^3 satisfies Eq. (22).
Generally, in *j*-th order of the scattering $\mathrm{R}^j = \sum_l \mathrm{E}_l^j + \mathrm{R}^{j+1}$

$$\mathrm{E}_l^j = -\mathbf{H}_l \mathbf{GW}_l \sum_{m \neq l} E_m^{j-1} \tag{24}$$

Then in point $\mathbf{x}$ of the medium the total *j*-th order component of the scattered field takes the form

$$E^j(\mathbf{x}) = -\sum_l \mathbf{GW}_l \mathrm{E}_l^j(\mathbf{x}') \qquad \mathbf{x}' \in \upsilon_l \tag{25}$$

The total scattered field is given by sum of the $E^j(\mathbf{x})$.
We obtain the discrete (numerical) representation of the above procedure when W is replaced by the weight system $W(j_l)$ for numerical integration's respect sampling structure vector $\mathbf{x} \rightarrow \mathbf{x}(j_l)$. Where j_l is the sample index in *l*-th element of the scattered structure.

5. RESULTS

The skeleton of the model of trabecular bone structure, applied in scattering field calculations, is presented in Fig.1(a). One of skeleton structures parallel to the x-z plane (horizontal respect incident field) is shown in Fig.1(b). The cylinder with Φ and length d was adopted as the model of trabecular. Each segment of the skeleton is the axis of cylinder.
The skeleton was obtained randomly by displacement of nodes in each layers of regular structure built of cuboids. Their dimensions are 2mm in the **y** direction and 1×1 mm in the **x** and **z** directions. The uniform probability was assumed for displacements in range (-0.15; 0.15) mm. The horizontal structures were adjusted to new node positions. Then some elements were randomly (uniform probability) eliminated from the structure. The results are similar to those which were presented in [6].

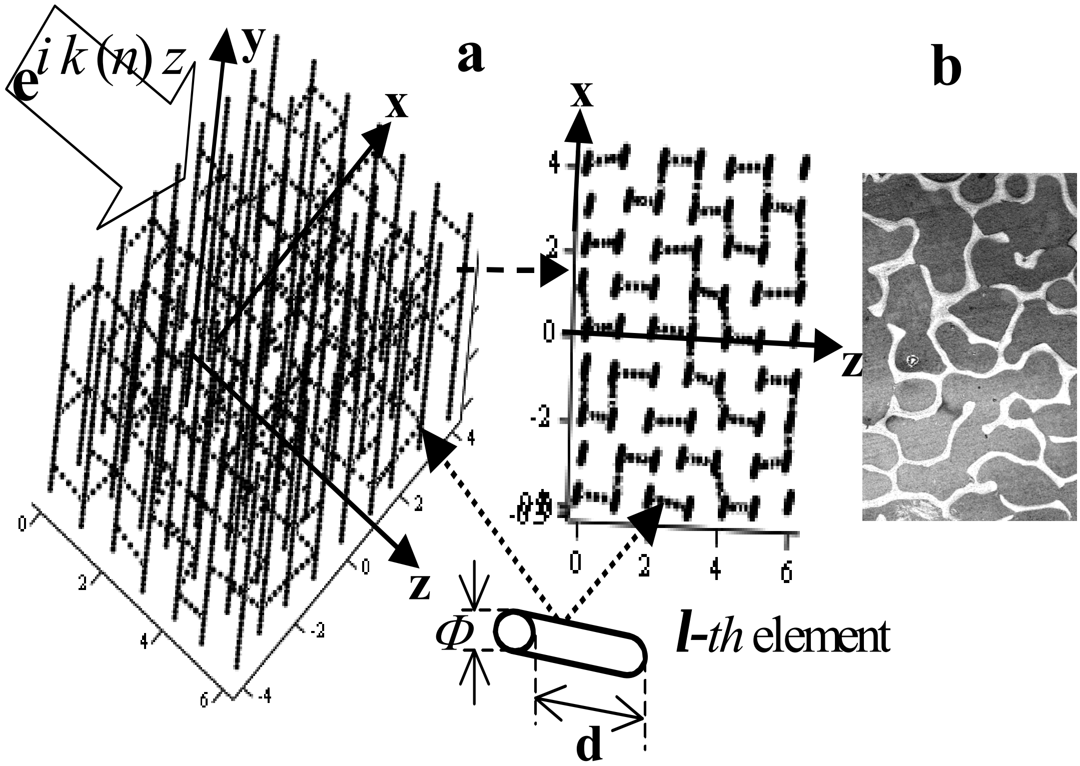

Fig.1. (**a**) left: full skeleton of the trabecular bone model; right: one of horizontal substructures in the skeleton. (**b**) the cross-section of the real trabecular bone structure

Values of sound speed and densities of each trabecualr were selected based on Gamma distribution. Maximum deviation from mean values 4000 m/s and 2000 kg/m^3 was assumed as ±5%. For trabecular, in ***y*** direction and in horizontal planes, mean values Φ=0.05 and 0.04 mm with deviations ±20% and ±25% respectively, were assumed.

For surrounding medium (marrow - fluid filler) as well as surrounding space g_0 = 1000kg/m^3, c_0=1500m/s. The absorption parameter for fluid filer was $2.3 \cdot 10^{-4}$ Np/mHz. Total number of elements (trabecular) was 409.

The unit plane wave was assumed as incident field $C^0 = \exp(ik(\nu)z)$ $z \geq 0, \nu \in [0.5, 3]$ MHz with step 0.333 MHz . Dimensionless frequency is $n = 15,16,...,90$.

5.1. SCATTERING FIELD DISTRIBUTION

Exemplary distributions of scattering fields in subsequent orders and for selected frequencies were shown in Fig.2. Brightness refers logarithmic scale of values. Contour of the scattering structure and its location is shown by white rectangle whereas white narrow indicates direction of incident wave. The represented area is the rectangle with location[-30,20]mm in ***z*** direction and [-15, 15]mm in ***x*** direction.

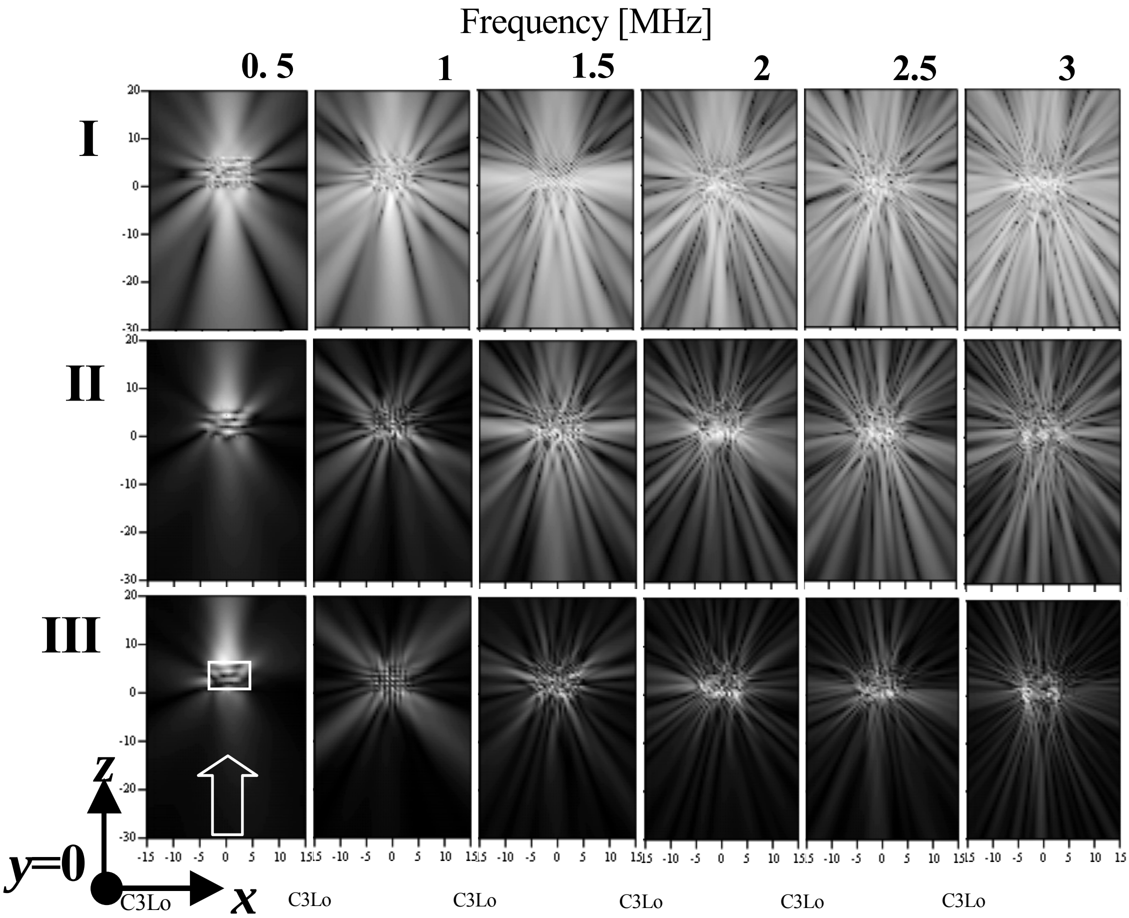

Fig.2. Distributions of fields in subsequent orders of scattering in rows: I, II, III, while in function of frequency from 0.5 MHz to 3 MHz they are shown in columns

5.2. BACKSCATTER COEFFICIENTS.

We define substructures: horizontal (denoted by "h") as a set of all trabecular that are situated in planes being parallel to the ***x-z*** plane, and vertical (denoted by "y') as a set of all trabecular which are parallel to the ***y*** axis.

In Fig.3 S is a sum of S1, S2 and S3, the effective backscatter cross-section coefficients, that were obtained in subsequent orders of scattering and in function of frequency ν. Multiplication factors, 50 and 5000, were applied for better representation. In the nearness of frequency ν=1.5 MHz, the estimated relations between values S1:S2:S3 from Fig.3 are as 1:(0.01):(0.0001). The S1,2,3 are characteristics of the second order in respect to field. In case of characteristics linear in respect to field the proportions will be as 1:(0.1): (0.01) or even higher.

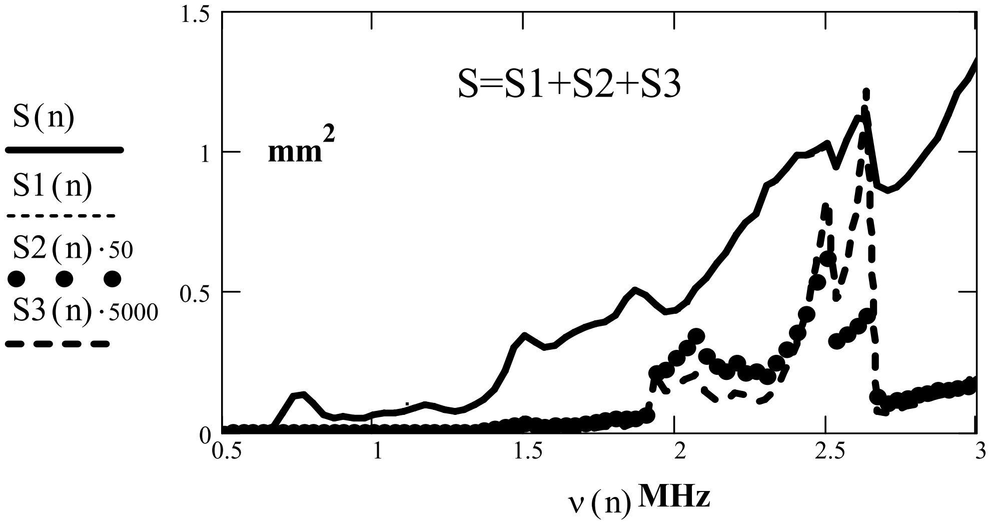

Fig.3. Effective backscatter cross-section decomposition in respect to scattering order

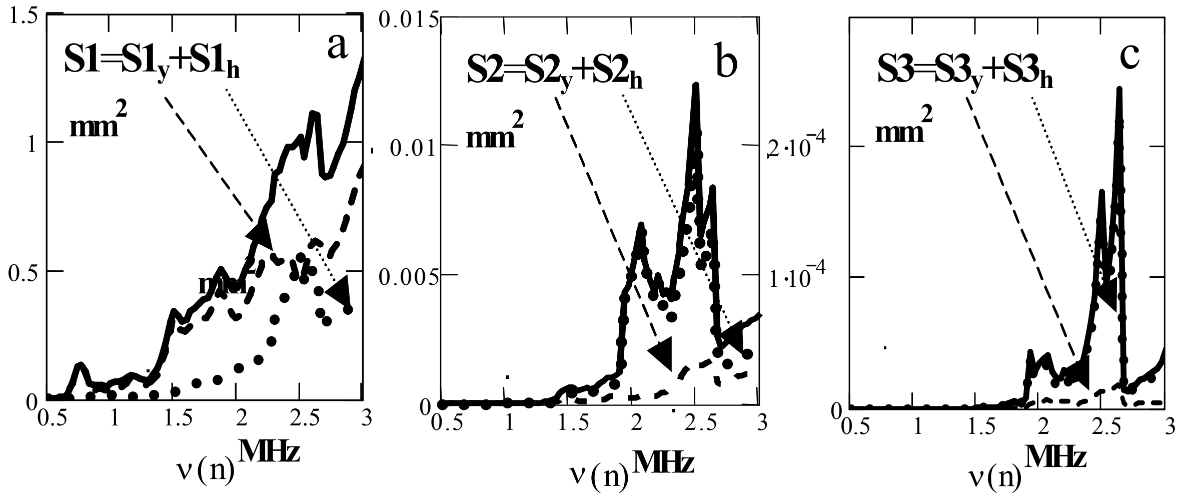

Fig.4. Contribution of substructures **h** and **y** in subsequent orders of scattering as well as in respect to frequency

In Figure 4. a, b, c the contribution of substructures **h** and **y** to effective backscatter cross-sections in subsequent orders of scattering is presented. Let us notice the validity change of substructures in transition from the first order to higher orders of scattering. It is visible in Figure 4.a and Figure 4.b (the transition occurs for ν>1.3 MHz).

In Fig.4.a the resonance for ν=0.75 MHz is observed. It is fully created by ***y*** substructure in which the trabecular length is 2mm. It corresponds to the resonance frequency. Similar analysis can be performed for other resonances using higher scattering orders.

6. CONCLUSIONS

In space-frequency range the method of solving of longitudinal wave scattering equations has been developed. It is convergent for high potentials and multi-element structures in numerical applications. The method is accurate in each order of scattering that means the calculated fields in subsequent order do not make corrections in scattering fields of former order. The Neuman's iteration of integral equations of scattering produce the asymptotically converged series (if it is converging); this means that each subsequent element of series includes improving accuracy corrections to former elements for the selected structure element. The developed algorithm enables the analysis of the scattering field characteristics taking into account not only the scattering order but also the influence of selected substructures. The examples of this effect has been presented.

In the range up to 1.5 MHz the influence of higher scattering orders on characteristics of the first order in respect to the field is less than few percent. In the range above 1.5 MHz one can observe in higher orders even several percent resonance effect of scattering.

ACKNOWLEDGEMENT

This work is supported by Ministry of Science and Higher Education (grant No. 0219/T02/2007/32).

REFERENCES

[1] K.Wear, Frequency dependence of ultrasonic backscatter from human trabecular bone: theory and experiments , J.Acoust. Soc.Am., 106(6),3659-3664, 1999.

[2] E.Bossy, F.Padilla, F.Peyrin, and P.Laugier, Three-dimensional simulation of ultrasound propagation through trabecular bone structures measured by synchrotron micro-tomography, Phys. Med. Biol.,vol.50, 5545-5556, 2005.

[3] K.Wear, Ultrasonic Scattering from Cancellous Bone: A review, IEEE Trans. Ultrason. Freq. Contr., vol.55,no.7, 1432-1441,2008.

[4] L.M.Brekhovskikh, O.Godin, Acoustics of Layered Media I, ISBN 3-540-51038-9 Springer-Verlag Berlin Haidelberg New York, 1-14, 1990.

[5] J.Wójcik, Conservation of energy and absorption in acoustic fields for linear and nonlinear propagation, J.Acoust.Soc.Am. 104 (5), 2654-2663, November 1998.

[6] A.Hosokawa, Development of Numerical Cancellous Bone Model for Finite-Difference Time-Domain Simulations of Ultrasound Propagation, IEEE TRANSACTIONS ON ULTRASONIC, FERROELECTRICS, ANDFREQUENCY CONTROL, vol.,55,no. 6, JUNE 2008